NANO LETTERS

Field-Dependent DNA Mobility in 20 nm High Nanoslits

Georgette B. Salieb-Beugelaar,*,§ Juliane Teapal,†,§ Jan van Nieuwkasteele,
Daniël Wijnperlé, Jonas O. Tegenfeldt,‡ Fred Lisdat,† Albert van den Berg,
and Jan C. T. Eijkel

*BIOS/Lab-on-a-Chip Group, MESA+ Institute for Nanotechnology, University of
Twente, P.O. Box 217, 7500 AE Enschede, The Netherlands, Biosystems Technology,
Wildau University of Applied Sciences, Germany, Department of Physics/Solid State
Physics, Lund University, Sweden*

ABSTRACT

The transport behavior of λ-DNA (48 kbp) in fused silica nanoslits is investigated upon application of electrical fields of different strengths.
The slit dimensions are 20 nm in height, 3 μm in width, and 500 μm in length. With fields of 30 kV/m or below, the molecules move fluently
through the slits, while at higher electrical fields, the DNA molecules move intermittently, resulting in a strongly reduced mobility. We propose
that the behavior can be explained by mechanical and/or field-induced dielectrophoretic DNA trapping due to the surface roughness in the
nanoslits. The observation of preferential pathways and trapping sites of the λ-DNA molecules through the nanoslits supports this hypothesis
and indicates that the classical viscous friction models to explain the DNA movement in nanoslits needs to be modified to include these
effects. Preliminary experiments with the smaller Xbal-digested litmus-DNA (2.8 kbp) show that the behavior is size-dependent, suggesting
that the high field electrophoresis in nanoslits can be used for DNA separation.

Introduction. The investigation of the behavior of confined DNA in a nanofluidic environment offers a promising way to explore its physical and structural properties.[1–10] This forms a basis for new devices for DNA analysis, to improve diagnostics, or to develop tools for the study of DNA−protein interactions.[11,12] General reviews useful in this context on DNA separation,[13,14] and on nanofluidics and nanotechnology[15–17] have been published.

DNA in a microfluidic environment will have a characteristic 3D "blob" shape. In a 2D nanofluidic environment ("nanoslit"), it will not be able to take this shape but instead must form a 2D pancake shape.[18,19] In a 1D nanofluidic environment, finally, DNA must stretch to a 1D "wormlike" molecule.[20] These nanofluidic conformations of DNA have been widely investigated in many different ways and explained with classical viscous friction models. Examples of phenomena observed are the compression and free expansion of single DNA molecules in nanochannels[21] or the analysis of the conformation while the biopolymer is undergoing an entropically induced motion.[5] Still unexplained behavior of this molecule was recently described[22] when

* Corresponding author. E-mail: g.b.salieb-beugelaar@ewi.utwente.nl
(G.B.S.-B.). Telephone: +31-53-4892755 (G.B.S.-B.).
† Biosystems Technology, Wildau University of Applied Sciences.
‡ Department of Physics/Solid State Physics, Lund University.
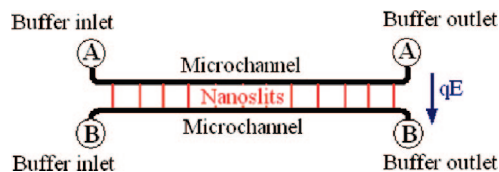§ Both authors contributed equally to this paper

Figure 1. Top view of the fused silica device. Between the microchannels, an array of 100 nanoslits is situated. Each nanoslit is facing at both sides the microchannels. The dimensions of the nanoslits are 3 μm in width, 500 μm in length, and a height of 20 nm.
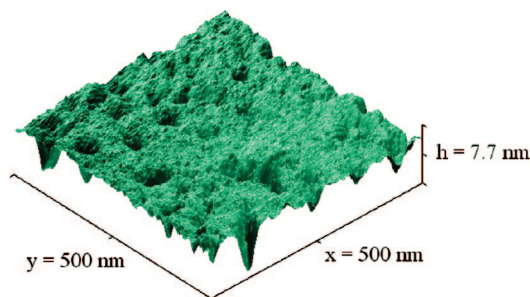

Figure 2. Surface roughness of the nanoslits as measured by AFM and using tips with a radius of 2 nm. Although the rms value is between 0.8 and 1.1 nm, holes occur with a depth of down to 8 nm.

silicon dioxide−glass nanoslits were used and a spontaneous stretching and attraction of DNA to the sidewall of the slits was found. Apart from the conformation, the mobility of DNA in a nanofluidic environment has also been investigated several times. Recent papers report size-dependent mobility and possibly the start of the development of new gel-free, size-dependent separation devices.[23,24] In the study presented here, we investigate the field-dependent mobility of DNA in 20 nm high nanoslits. We show that manipulation of the electrical field can strongly influence DNA mobility and offer as a possible explanation of the observed behavior dielectrophoretic and/or steric trapping.

Experimental Methods. Device Fabrication. The nanoslit devices were manufactured in fused silica (Figure 1). The dimensions of the chip are 10 mm × 20 mm, and it is composed out of two fused wafers. In one wafer, an array of 100 parallel nanoslits are manufactured by using standard photolithography and etching in a buffered hydrogen fluoride (BHF) solution. The dimension of each nanoslit is 3 μm in width, 500 μm in length, and 20 nm in height. In the other wafer, two microchannels are manufactured by using standard photolithography and etching with 0.5% HF solution. The dimensions of the microchannels are 19 μm in height, 300 μm in width, and 12.5 mm in length. The four fluidic connection holes were manufactured by photolithography and powder blasting. Prior to bonding, the nanoslit and microchannel depth was measured. Also, the surface roughness in the nanoslits was studied. A typical AFM scan is shown in Figure 2. AFM tips were used with a radius of 7 and 2 nm. The rms roughness values were ranging from 0.8 to 1.1 nm. Holes in the surface, with a depth down to 8 nm, also occur, as can be seen in the AFM scan shown in Figure 2. The holes were already present before etching (AFM scans). After the AFM measurements the wafers were oxygen

plasma cleaned and fusion bonded at a temperature of 1100 °C. The bonding creates a connection between the microchannels by the intermediate array of nanoslits.

Buffer Solution A. Nonmethylated λ-DNA (48 kbp) or XbaI digested litmus 28i DNA (2.8 kp) (New England Biolabs) was labeled with the intercalating dye YOYO-1 (Invitrogen) at a ratio of 1:5 (dye:base pair). YOYO-1 increases the total length of λ-DNA to ∼21 μm.[25] The staining was done by adding both DNA and the YOYO-1 to 1× Tris borate sodium EDTA (TBE) buffer (pH = 8.3). The solution was incubated for at least 1 h at room temperature. DNA was diluted to a concentration of 400 ng/mL in 1× TBE containing 2.5% (w/w) polyvinylpyrrolidone (MW = 10000 Da) to suppress electroosmotic flow and 3% (v/v) β-mercaptoethanol to suppress photobleaching and photoknicking.[26] Before the experiments, the solution was degassed in vacuum.

Buffer Solution B. This buffer is composed of the same components as described for buffer solution A, except that no labeled DNA was added.

Electrical Potential Measurement. The resistance of the microchannels was negligible with respect to the resistance of the nanochannels. To measure the exact applied potential difference over the nanoslit array, a potentiostat (Parstat 2263, Princeton Applied Research) and Ag/AgCl reference electrodes were used, which were placed in the buffer vials.

Experiments. In a continuous flow, buffer was pressure driven through the microchannels, as shown in Figure 1. Buffer A was driven into inlet A, whereas buffer B was driven into inlet B. The λ-DNA/litmus molecules were pulled into the nanoslits by applying electrical fields between 6 and 200 kV/m. Excitation of the YOYO-1 molecules was done by using a mercury lamp. DNA molecules were traced inside the nanoslits using a Leica microscope, a 63× objective, Leica L5 filter set, an Andor iXon EMCCD camera, and a frame rate of 5 frames per s. Image J[27] and MATLAB (The MathWorks, Natick, MA) were used to process and analyze the video files.

Results and Discussion. DNA translocation experiments were carried out at electrical fields of 6−200 kV/m. At low electrical fields (below 30 kV/m), a fluent movement of the λ-DNA molecules was observed. At high electrical fields (30 kV/m and above), an intermittent movement of λ-DNA molecules was observed. Figure 3 shows three successive video frames of λ-DNA molecules in a nanoslit. In this experiment, a high electrical field of 200 kV/m is applied.

One λ-DNA molecule (red area within a white circle) is moving in the three frames. The other, not moving yellow-red areas represent λ-DNA, which was permanently trapped during this experiment at high field. From the displacement of the DNA inside white circles, the mobility of the center of mass of the DNA was calculated. We found that the movement of the molecules differed as a function of the applied field. Figure 4 shows an example of an intermittent movement as a distance/time graph. Part A in this graph represents the movement during the three frames displayed in Figure 3. B represents the time in which the molecule was trapped. To study in detail the intermittent movement
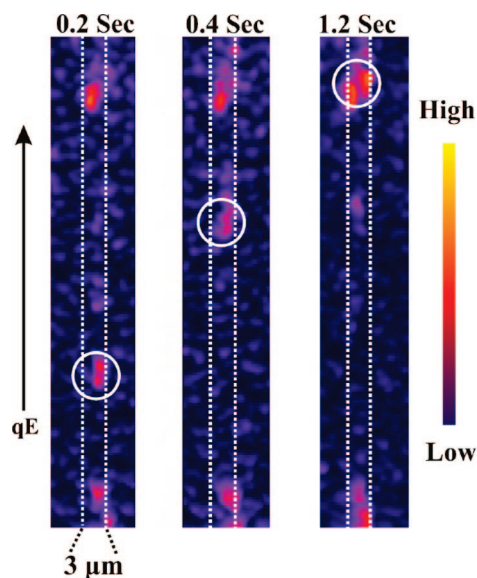
Figure 3. Example of a typical analysis of DNA movement is presented here in three different video frames. The number of frames during which an intermittently moving molecule would move vary between molecules. The tracked DNA is in the white circle. The color coding runs from yellow (high fluorescent emission) to blue (low fluorescent emission). Out of these data, plots as presented in Figure 4 were created to calculate DNA mobility.
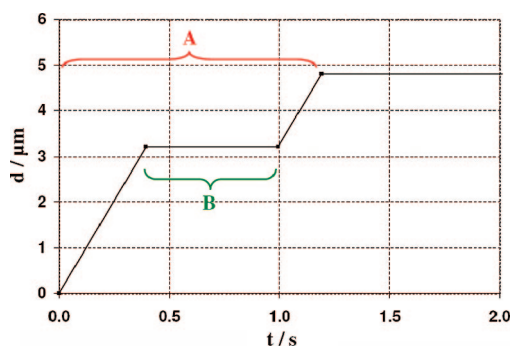

Figure 4. Intermittent movement of a single DNA molecule at a high electrical field of 200 kV/m. The data provided by the video frames of Figure 3 were used to calculate part A of this graph. Part B represents the time in which the molecule was trapped. Frame rate was 5 Hz.

and the possible occurrence of traps and preferential pathways, the video frames were superimposed. An example of these constructed pathways, from the video frames of the same experiment used in Figure 3, is shown in Figure 5. Traps of different strength were found. For example, traps existed where most λ-DNA molecules were delayed or temporarily trapped. Also, traps existed where some of the molecules got trapped, whereas other molecules moved through fluently. Possible explanations for the trapping mechanisms at the traps can be steric trapping or dielectrophoresis.[28,29] Steric trapping can occur at places were the surface roughness is so large that it causes a mechanical obstacle in the slit. DNA moving through the nanoslit as a result of the applied electrical field meets the obstacle and is pulled into, around, or against it by the electrical field, in this way trapping the molecule.[30] It subsequently will depend on the shape of the obstacle and the strength of the electrical
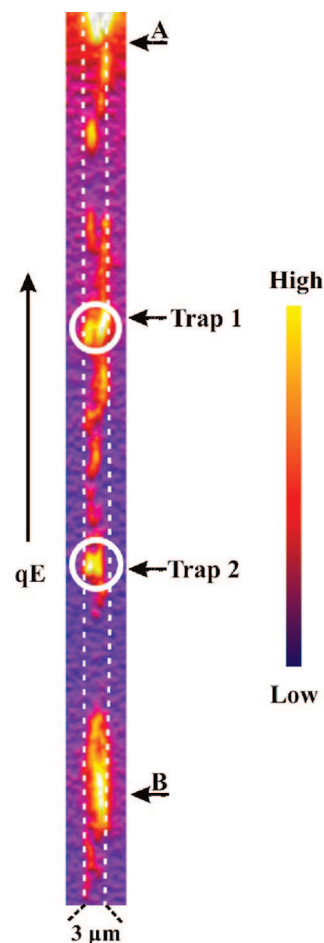

Figure 5. By superimposing all the frames of one movie, the pathways of the DNA molecules can be tracked inside a particular part of a nanoslit. Again, the same movie as in Figure 3 is taken. A is the exit of the nanoslit, whereas at the location of B, molecules remained permanently trapped during this experiment. The white circles represent trap 1 and trap 2 inside the nanoslit where the molecules were trapped for a particular time and then continued moving. Interestingly, the molecules seem to follow preferred pathways inside these nanoslits. At trap 1 and trap 2, molecules were transiently trapped.

field, whether the λ-DNA is able to escape, which will only be possible due to the thermal movement (diffusion). This type of trapping is expected to be highly field-dependent,[31] as indeed observed. Alternatively, the behavior of temporary trapping may be explained by dielectrophoresis. Because of the roughness of the surface (for example, the holes visible at the AFM scan in Figure 2), the electrical field will be nonuniform inside the nanoslits, resulting in high local electrical field gradients. By dielectrophoresis, charged molecules can be trapped at such places, and the higher the electrical field, the more difficult it is to escape out of these traps. In microchannels the trapping of DNA molecules by dielectrophoresis has been reported in several papers.[32−35] Ajdari and Prost[31] predicted an exponential dependence of the trapping time on the electrical field strength. A combination of both steric trapping and dielectrophoresis at sites of surface roughness is also possible.

In the view of the above, we calculated the mobility at different applied fields from λ-DNA molecules movement.
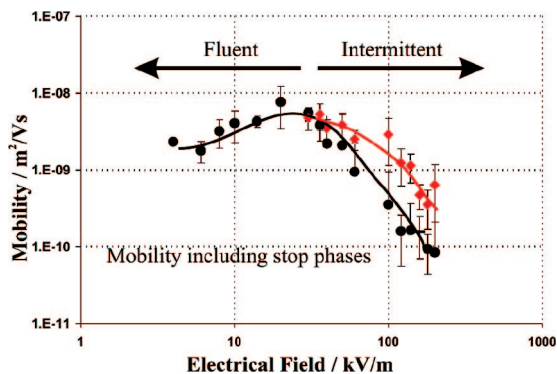
Figure 6. Mobilities of λ-DNA molecules in different applied fields. Each datapoint corresponds to an average over 10 or more λ-DNA molecules. At fields lower than 30 kV/m, the movement of the molecules is fluent, whereas above 30 kV/m, the movement is intermittent. For the intermittent movements, we have calculated two different mobilities: first, an overall mobility in which we include the trapping time (black line) and, second, a mobility calculated only from the movements (red line). The lines drawn are only an indication for the eye. Error bars represent the standard deviation.

For the fluent movements at low applied fields, a direct calculation of the mobility was possible, while for the intermittent movements, two different values of the mobility were calculated, namely an overall mobility that included the trapping times and a mobility for the movement phases alone. Important to mention is the limited frame rate (5 Hz) we used, which causes an underestimation of the mobility determined for the intermittent movement. Another source of error for the mobility data is that a fraction of molecules did not move during the entire duration of the experiment (typically 60 s). This fraction increased with increasing applied electrical field. These molecules were not included in the data used to calculate the mobility. The true average mobility will for this reason be even lower than calculated. Figure 6 displays an overview of the mobilities measured at all applied fields. We will compare our results with the free solution mobility and the mobilities of DNA inside the nanoslits as reported by Cross and co-workers.[23]

The experiments in Cross' investigation were performed at low electrical fields (2−6 kV/m) in (partly) 19 nm high nanoslits. The free solution mobility they found was 1.1×10^{-8} m²/Vs (8 kb DNA molecules), whereas the mobility for λ-DNA in the nanoslit extrapolated from their equation for our longer DNA length would be 7.2×10^{-9} m²/V s. In the electrical fields below 30 kV/m we saw fluent movement. The mobilities we found are about a factor of 2 smaller than the ones extrapolated from the data of Cross and co-workers.[23] Because the fields we applied are comparable, similar mobilities would be expected. Possible explanations for the low mobility we found can be a difference in surface roughness as a result of the used fabrication method, the fact that Cross' equation cannot be extrapolated to longer DNA lengths, or different levels of residual EOF (Cross used a lower PVP concentration). Above 30 kV/m, the mobility decreases rapidly and a transition from fluent movements to intermittent movement is seen. The mobility calculated from the movement phases decreases to 5% of the free solution
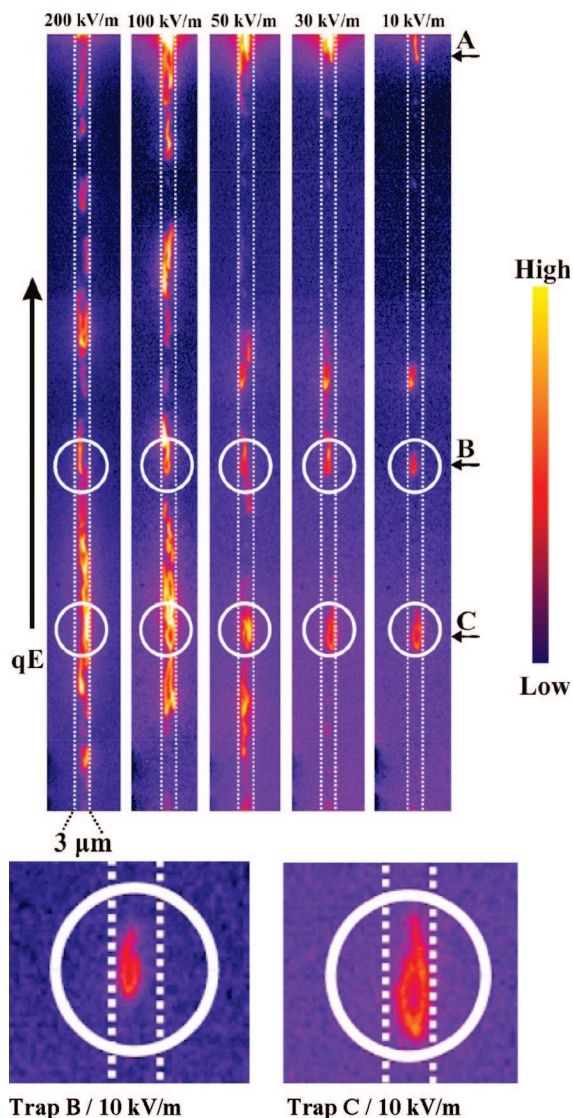

Figure 7. By superimposing 300 consecutive frames of experiments at different applied electrical field strength, the trapping of λ-DNA in one nanoslit can be studied. A is the exit of the nanoslit. The other white circles (B and C) are examples of traps. Most λ-DNA was temporary delayed or trapped at these places when electrical fields of 30 kV/m and above are applied.

mobility at 200 kV/m, whereas the overall mobility when the trapping times are included is only 1% of the free solution mobility. To our knowledge, such a strong field-dependent mobility has not been reported before in literature, or even been observed in gels. To investigate the field-dependent trapping inside the nanoslits in more detail, frames of experiments at different applied electrical fields were superimposed in the same way as for Figure 5 (Figure 7). The experiment shown started at high electrical field to pull the λ-DNA molecules into the nanoslits. In Figure 7, A indicates the exit of the nanoslit, whereas B and C show examples of traps. Clearly, in fields of 50 kV/m and above, more λ-DNA molecules are trapped in the nanoslit and at more locations. When the field subsequently was decreased, molecules were less and less trapped. In a few traps, however, λ-DNA molecules remained trapped also at the low voltages. Detailed pictures of DNA in trap B and C at 10 kV/m show hook-

shaped λ-DNA molecules, which were not able to escape out of these traps during the entire experiment (and thus were not included in the calculations). At applied electrical fields of higher than 30 kV/m, λ-DNA molecules were delayed or trapped at B and C. When an electrical field of 10 kV/m was applied, λ-DNA molecules were not delayed or trapped at B and C anymore but were able to flow fluently through the entire part of the nanoslit. Important to mention is that during these experiments we found no proof of breaking of λ-DNA molecules. Besides the field dependence of DNA movement in the region of intermittent movement, it was also investigated how the field is influencing the mobility in the region of fluent movement. Surprisingly, here a decrease of mobility was found as the electrical field is decreased from 30 to 6 kV/m (see Figure 6), although the change is much smaller than in the high field range. At present, we have no explanation for this behavior, which seems to be significant in view of the standard deviation of the data determined.

It was investigated whether the observed field-dependent behavior was different for another type of DNA molecule namely litmus DNA (digested with XbaI, 2.8 kbp). In that case, the field-dependent mobility could offer a method for separating DNA of different lengths. Parts A and B in Figure 8 compare the mobility of λ-DNA with preliminary results for the mobility of litmus DNA (XbaI digested). Figure 8A shows that the overall mobility for λ-DNA is considerably higher than the overall mobility of litmus DNA. This behavior could thus indeed be a basis for DNA separations. Figure 8B shows that also the mobilities during the moving phases differ, that of λ-DNA being higher. Such behavior is as yet unexplained, but possibly transient trapping of parts of the molecule play a role. We observed that even at an applied electrical field of 6 kV/m, litmus DNA moved in an intermittent way. Thus, the shorter litmus DNA is still trapped at electrical fields where the longer λ-DNA moves in a fluent way through the nanoslits. This behavior could possibly be explained by dielectrophoretic trapping if it is assumed that the dielectrophoretic traps are smaller than the size of λ-DNA but closer to the dimensions of litmus DNA. In that case, the larger λ-DNA will be able to escape more easily than the litmus DNA at high applied electrical field because a smaller part of the λ-DNA molecule is trapped by dielectrophoresis than the litmus DNA. We plan to investigate this phenomenon in more detail in the future because differences in field-dependent mobility could enable separation of DNA. Especially, the ease with which an applied field can be changed would offer a great advantage for separations, offering a convenient control parameter.

Conclusion. To our knowledge, we report for the first time a field-dependent mobility of λ-DNA molecules in nanoslits. At low electrical fields (below 30 kV/m), a fluent movement was seen and the mobility was only slightly lower than the free solution mobility of Cross and co-workers.[23] At electrical fields of 30 kV/m and above, an intermittent movement as well as a strongly field-dependent trapping of the DNA was observed, resulting in a strong reduced mobility at high fields. Preliminary results show a difference in trapping behavior of λ-DNA and litmus DNA, which can possibly be explained
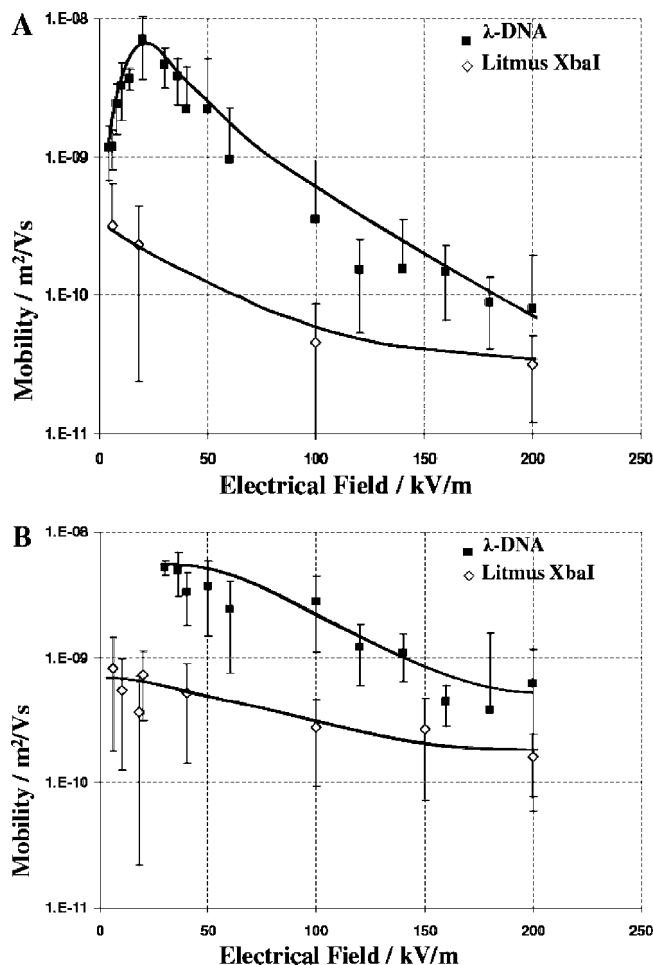

Figure 8. In A, the overall mobility of λ-DNA and litmus DNA (XbaI digested) is presented. The preliminary data of litmus DNA show already that the overall mobility is much lower than for λ-DNA. In B, the mobility calculated only from the moving phases between trapping events is presented. Litmus DNA (XbaI digested) moves in an intermittent way at electrical fields from 30 down to 6 kV/m, where λ-DNA molecules move fluently through the nanoslits. The lines drawn are only an indication for the eye. Error bars represent the standard deviation.

by dielectrophoretic trapping. Together with the recently published size-dependent DNA mobility in nanochannels of Cross and co-workers,[23] the observed behavior can open doors to the development of new gel free separation devices.

References
(1) Reisner, W.; Morton, K. J.; Riehn, R.; Wang, Y. M.; Yu, Z.; Rosen, M.; Sturm, J. C.; Chou, S. Y.; Frey, E.; Austin, R. *Phys. Rev. Lett.* **2005**, *94*, 196101.
(2) Tegenfeldt, J. O.; Prinz, C.; Cao, H.; Chou, S.; Reisner, W. W.; Riehn, R.; Wang, Y. M.; Cox, E. C.; Sturm, J. C.; Silberzan, P.; Austin, R. H. *Proc. Natl. Acad. Sci. U.S.A.* **2004**, *101*, 30.

(3) Balducci, A.; Mao, P.; Han, J.; Doyle, P. S. *Macromolecules* **2006**, *39*, 6273.

(4) Lin, P. K.; Fu, C. C.; Chen, Y. L.; Chen, Y. R.; Wei, P. K.; Kuan, C. H.; Fann, W. S. *Phys. Rev. E* **2007**, *76*, 1806.

(5) Mannion, J. T.; Reccius, C. H.; Cross, J. D.; Craighead, H. G. *Biophys. J.* **2006**, *90*, 4538.

(6) Reccius, C. H.; Mannion, J. T.; Cross, J. D.; Craighead, H. G. *Phys. Rev. Lett.* **2005**, *95*, 268101.

(7) Hsieh, C. C.; Balducci, A.; Doyle, P. S. *Macromolecules* **2007**, *40*, 5196.

(8) Campbell, L. C.; Wilkinson, M. J.; Manz, A.; Camilleri, P.; Humphreys, C. J. *Lab on a Chip* **2004**, *4*, 225.

(9) Fu, J.; Mao, P. *Appl. Phys. Lett.* **2005**, *87*, 263902.

(10) Riehn, R.; Austin, R. H.; Sturm, J. C. *Nano Lett.* **2006**, *6*, 1973.

(11) Wang, Y. M.; Tegenfeldt, J. O.; Sturm, J.; Austin, R. H. *Nanotechnology* **2005**, *16*, 1993.

(12) Wang, Y. M.; Tegenfeldt, J. O.; Reisner, W.; Riehn, R.; Guan, X. J.; Golding, I.; Cox, E. C.; Sturm, J.; Austin, R. H. *Proc. Natl. Acad. Sci. U.S.A.* **2005**, *102*, 28–9796.

(13) Viovy, J. L. *Rev. Mod. Phys.* **2000**, *Vol. 72, No. 3*, 813.

(14) Slater, G. W. *Electrophoresis* **2002**, *23*, 3791.

(15) Eijkel, J. C. T.; van den Berg, A. *Electrophoresis* **2006**, *27*, 677.

(16) Eijkel, J. C. T.; van den Berg, A. *Lab on a Chip* **2006**, *6*, 1–19.

(17) Tegenfeldt, J. O.; Prinz, C.; Cao, H.; Huang, R. L.; Austin, R. H.; Chou, S. Y.; Cox, E. C.; Sturm, J. C. *Anal. Bioanal. Chem.* **2004**, *378*, 1678.

(18) Brochard, F. *J. Phys.* **1977**, *38*, 1285.

(19) Brochard, F; de Gennes, P. G. *J. Chem. Phys.* **1977**, *67*, 52.

(20) Odijk, T. *Macromolecules* **1983**, *16*, 1340.

(21) Reccius, C. H.; Mannion, J. T.; Cross, J. D.; Craighead, H. G. *Phys. Rev. Lett.* **2005**, *95*, 268101.

(22) Krishnan, M.; Mönch, I.; Schwille, P. *Nano Lett.* **2007**, *7*, 1270.

(23) Cross, J. D.; Strychalski, E. A.; Craighead, H. G. *J. Appl. Phys.* **2007**, *102*, 024701.

(24) Pennathur, S.; Baldessari, F.; Santiago, J. G.; Kattah, M. G.; Steinman, J. B.; Utz, P. J. *Anal. Chem.* **2007**, *79*, 8316.

(25) Reisner, W.; Beech, J. P.; Larsen, N. B.; Flyvbjerg, H.; Kristensen, A.; Tegenfeldt, J. O. *Phys. Rev. Lett.* **2007**, *99*, 058302.

(26) Åkerman, B.; Tuite, E. *Nucleic Acid Res.* **1994**, *24*, 1080.

(27) Rasband, W. *Image J*, version 1.37; National Institutes of Health: Bethesda, MD; 2006; http://rsb.info.nih.gov/.

(28) Regtmeier, J.; Duong, T. T.; Eichhorn, R.; Anselmetti, D.; Ros, A. *Anal. Chem.* **2007**, *79*, 3925.

(29) Asbury, C. L.; Diercks, A. H.; van den Engh, G. *Electrophoresis* **2002**, *23*, 2658.

(30) Gauthier, M. G.; Slater, G. W. *J. Chem. Phys.* **2002**, *117*, 6745.

(31) Ajdari, A.; Prost, J. *Proc. Natl. Acad. Sci. U.S.A.* **1991**, *88*, 4468.

(32) Chou, C. F.; Tegenfeldt, J. O.; Bakajin, O.; Chan, S. S.; Cox, E. C.; Darnton, N.; Duke, T.; Austin, R. H. *Biophys. J.* **2002**, *83*, 2170.

(33) Tuukkanen, S.; Toppari, J. J.; Kuzyk, A.; Hirviniemi, L; Hytönen, V. P.; Ihalainen, T.; Törmä, P. *Nano Lett.* **2006**, *6*, 1339.

(34) Bakewell, D. J.; Morgan, H. *IEEE Trans. Nanobiosci.* **2006**, *5*, 1.

(35) Nagahiro, S.; Kawano, S.; Kotera, H. *Phys. Rev. E* **2007**, *75*, 011902.

NL080300V